Rare Metal Materials and Engineering
Volume 52, Issue 10, October 2023
Available online at www.rmme.ac.cn

Science Press

Cite this article as: Cui Shushan, Shi Tao, Lu Chao, et al. Phase-Field Study of Low-Temperature Decomposition Mechanism in U-Nb Alloys[J]. Rare Metal Materials and Engineering, 2023, 52(10): 3374-3381.

ARTICLE

Phase-Field Study of Low-Temperature Decomposition Mechanism in U-Nb Alloys

Cui Shushan, Shi Tao, Lu Chao, Yin Jiaqing, Su Bin

Institute of Materials, China Academy of Engineering Physics, Jiangyou 621907, China

Abstract: The microstructure evolution responsible for significant change of mechanical properties during low-temperature aging of U-Nb alloys was investigated by phase-field method. Results show that spinodal decomposition may occur at the early stage only when its thermodynamic condition is satisfied. Possibilities of general precipitation widely exist at low-temperature region, where the Nb content difference between the stable nucleus and the matrix can be significantly small, no matter the matrix of aging is cubic-like phase or in the orthorhombic-like phase, because the alloy composition is close to the critical composition of structural transition. At low diffusion rate and the relatively high mobility of phase interface, the Nb content of growing precipitates is far away from equilibrium composition. It is suggested that the Nb redistribution caused by phase decomposition may be responsible for the low-temperature aging hardening effect in U-Nb alloys.

Key words: U-Nb alloy; low-temperature aging; phase-field simulation

As-quenched U-Nb alloys are widely used in nuclear industries due to their outstanding properties of corrosion resistance and ductility[1–3]. However, the corresponding feature of Nb supersaturation may result in unacceptable performance degradation after long-term natural or artificial aging. Therefore, the low-temperature aging of U-Nb alloys has received abundant attention for the last two decades. It is reported that the yield and ultimate strengths of U-14Nb (at%) alloy increases after 20 a of natural aging, but the tensile elongation does not decrease[4]. Hackenberg et al[5] obtained a series of tensile data about the influence of aging temperature (from 373 K to 573 K) and time (from 10 min to 5 a) on the mechanical properties of as-quenched U-13.2Nb and U-17.6Nb alloys. On the whole, the strengths increase and the ductility decreases with aging time. The rate of property change increases with increasing temperature, indicating that a thermally activated phase decomposition mechanism may be responsible for the aging effect. Nano-scale Nb redistribution was observed by atom probe tomography in U-13Nb alloy aged at 573 K for 70 d, but no evident Nb segregation was observed when aged at 473 K for 70 d[6]. For the later condition, the increase in first-yield strength is higher than 500 MPa, and the elongation has decreased from 0.2 to <0.05[5]. Therefore, the detailed phase decomposition process, which is responsible for the aging strengthening effect of U-Nb alloys, is still unclear and needs to be further confirmed.

Compared to numerous experimental studies, insufficient theoretical analysis of low-temperature aging effect in U-Nb alloys can be found in the literature. Clarke et al[6] analyzed the possibility of spinodal decomposition via a relatively simple thermodynamic model, and the results indicate that spinodal mechanism is unlikely for U-13.2Nb alloy aged at temperatures lower than 573 K. They also calculated the characteristic diffusion length based on the phenomenological activation energy, and the results do not support the idea of diffusion-driven decomposition mechanism. Considering that only simple thermodynamic and diffusion calculations were made, their conclusions may be questionable and need further validation. Currently, several researchers[7–11] reported their thermodynamic and kinetic diffusivity models for U-Nb system by means of CALPHAD (calculation of phase diagrams). Nevertheless, these models have not yet been applied to investigate the issue of low-temperature phase decomposition.

Although the phase diagram can provide the information of ultimate decomposition products, sometimes it cannot

Received date: March 05, 2023
Foundation item: National Natural Science Foundation of China (51901210); Project Supported by CAEP Foundation (CX20210008)
Corresponding author: Su Bin, Ph. D., Associate Professor, Institute of Materials, China Academy of Engineering Physics, Jiangyou 621907, P. R. China, Tel: 0086-816-3626130, E-mail: sub703@126.com

correctly predict the decomposition mechanism when the system is far away from the equilibrium state. This problem has been largely overcome by the development of phase-field simulation, which is widely used to theoretically investigate the microstructure evolution of solidification and solid-state phase transformation[12–15]. Phase-field modeling belongs to the mesoscopic continuum methods of materials computation, and the phase interface is treated as diffuse, rather than sharp. The temporal microstructure evolution is controlled by the principle of Gibbs free energy minimization. With the fundamental thermodynamic and kinetic information as the input, phase-field method is able to simulate the formation process of transformation products. Duong et al[16] successfully applied the phase-field method to simulate the reaction of discontinuous precipitation in U-Nb alloys. Wang et al[17] used the phase-field model to elucidate the effect of Nb content on the morphology of spinodal decomposition in Zr-Nb alloys. Liu et al[18] developed a phase-field model to simulate the homogeneous and heterogeneous formation of precipitates in Al-Cu alloys.

In this study, we carried out phase-field simulations to reveal the possible mechanism of phase decomposition during low-temperature aging in U-13.2Nb alloy. In detail, two aging temperatures, 573 and 423 K, were investigated. Several factors that influence the formed microstructure were analyzed, including the chosen thermodynamic data set, the nucleation rate, the diffusion coefficient and the intrinsic interface mobility.

1 Phase-Field Model

During rapid cooling from the solid-solution temperature to room temperature, the bcc γ phase starts to transform into $\gamma°$ at about 590 K for U-13.2Nb alloy, and this diffusionless transformation will complete within 20 K[19]. The $\gamma°$ phase is a tetragonally distorted version of γ. The $\gamma° \rightarrow \alpha''$ martensitic transformation starts at around 450 K, and will finish at around 400 K. The α'' phase is a monoclinically distorted version of the orthorhombic α phase. Unfortunately, the CALPHAD method has not been used to calculate the metastable phase diagram of U-Nb system, and thus the thermodynamic data for α'' and $\gamma°$ phases is currently absent. Considering the similarity of crystal structure, the α'' and $\gamma°$ phases are approximately treated as the α and γ phases, respectively.

According to the thermodynamic model of Liu et al[7], the Gibbs free energy vs composition curves at 573 K are shown in Fig. 1a. As the intersecting point indicates structural transformation, the derived relationship between transformation temperature and Nb content (Fig. 1b) is not consistent with experimental results[19]. In order to offset this discrepancy, a modification of the Gibbs free energy of α phase Nb is follows:

$$ {}^{0}G^{\alpha}_{\mathrm{Nb}} = {}^{0}G^{\gamma}_{\mathrm{Nb}} + (67100 - 23.8T) \tag{1} $$

Apparently, the α phase is more stable on the low Nb side, the γ phase is more stable on the high Nb side, and the free energy curve of α is simpler than that of γ. After modification,

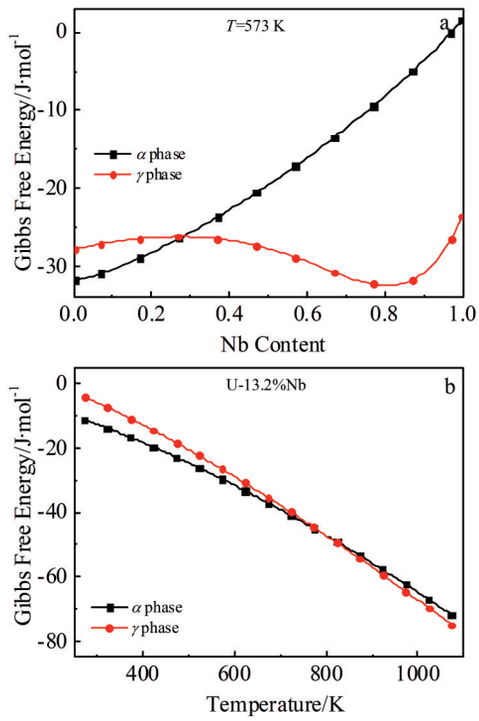

Fig.1 Curves of Gibbs free energy vs Nb content at 573 K (a) and Gibbs free energy vs temperature of U-13.2Nb alloy (b) for γ and α phases based on Liu's[7] thermodynamic data

the start temperature of structural transformation between α phase and γ phase derived from the Gibbs free energy curves is consistent with the experimental results of M_s from $\gamma°$ phase to α'' phase[19].

In general, the phase-field model of phase decomposition should take both the composition and structure fields into account. Here, we assumed a strong correlation between composition and structure, which means that the crystal structure is only dependent on the composition. Then, only the evolution of composition field needs to be described, which is governed by:

$$ \frac{\partial c(r,t)}{\partial t} = \nabla M \nabla \frac{\delta F}{\delta c(r,t)} \tag{2} $$

where c is the composition field, i. e. Nb content, M is the atomic mobility coefficient, and F is the total free energy of the system. In solid-state phase transformations, F usually includes the chemical energy (f_{ch}), the gradient energy (f_{gr}) and the elastic strain energy (f_{el}):

$$ F = \int_V (f_{\mathrm{ch}} + f_{\mathrm{gr}} + f_{\mathrm{el}}) \mathrm{d}V \tag{3} $$

The chemical energy is a piecewise function to composition:

$$ f_{\mathrm{ch}} = \min\left(G_{\gamma}(c), G_{\alpha}(c)\right) \tag{4} $$

where G is the Gibbs free energy, obtained from the CALPHAD model. Smoothing of f_{ch} is applied in order to guarantee its first-order continuity. The gradient energy is expressed as:

$$ f_{\mathrm{gr}} = \frac{\beta}{2} (\nabla c)^2 \tag{5} $$

where β is the gradient coefficient. The elastic strain energy is

dependent on the composition difference between the decomposed products and the parent phase[6], and is given as:

$$f_{el} = \eta^2 (c - c_0)^2 E' V_m \quad (6)$$

where η is the fractional change in lattice parameter per unit composition change; $E' = E/(1-\nu)$, E is the elastic modulus and ν is the Possion's ratio; V_m is the molar volume; c_0 is the initial Nb content. M is is given as[17]

$$M = c_{Nb} c_U (c_{Nb} M_U + c_U M_{Nb}) \quad (7)$$

Based on the CALPHAD framework, the atomic mobility of element k is given as

$$\Phi M_k = \frac{1}{RT} e^{\Phi_k / RT} \quad (8)$$

where Φ_k is dependent on composition and temperature[10]. For U-Nb system, the atomic mobility coefficients of γ' are available in the literature, but those of α are absent. The self-diffusion data indicate that the intrinsic diffusivity in α is obviously lower than that in γ[20], and thus a factor of crystal structure (m_c) is added.

Due to high computational cost for three-dimensional simulation, we carried out two-dimensional simulations, with 200×200 grids. The corresponding real length of a grid cell was chosen as 0.2 nm. Finite difference method was used to numerically solve the above phase-field equation, and the boundary condition was set as periodic. The input parameters are given in Table 1.

2 Results

2.1 Aging of γ phase at the spinodal region

According to the classical theory of phase transformation, the phase separation region of the γ phase can be divided into the metastable region and the unstable region. In the unstable region, the thermodynamic condition is satisfied, which means that there is no barrier for nucleation and spinodal decomposition occurs. In the metastable region, the classical nucleation-growth process is the decomposition mechanism. Furthermore, taking the elastic strain energy, resulted from the coherent lattice misfit between Nb-rich and Nb-lean regions, into account, the spinodal region can be further divided into the chemical and coherent spinodal regions. Based on two independent thermodynamic data sets[7,8], apparent difference is found between the calculated regions, as shown in Fig. 2. According to the calculated results, different thermodynamic data sets will result in different decomposition mechanisms at 573 K. Based on Liu's data, coherent spinodal is the mechanism at the early decomposition stage. However, based on Duong's data, spinodal decomposition will not occur. The first case is used in this section, and the second case is considered in the following section. Therefore, U-13.2Nb alloy is kept as γ phase at 573 K, and located in the coherent spinodal region.

Table 1 Input parameters for calculation[4,12]

Parameter	Value
β/×10^{-9} J·m^{-2}	1
E/GPa	68.9
ν	0.35
η	−0.074
V_m/×10^{-5} m^3·mol^{-1}	1.28

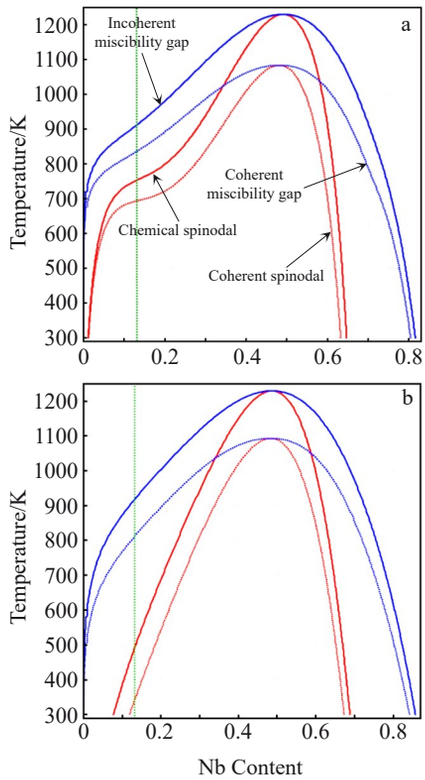

Fig.2 Divided decomposition regions of U-Nb alloy based on different thermodynamic data sets from Liu[7] (a) and Duong[8] (b)

Firstly, it was assumed that no structural transformation occurs during the decomposition process, i.e. the α phase was ignored. Random composition fluctuation was used as the initial condition, and Fig. 3 shows the simulated results of microstructure evolution aged at 573 K. The classical spinodal decomposition process can be found (Fig.3b), i.e. the "uphill" diffusion results in Nb redistribution, and the Nb difference between Nb-rich and Nb-lean regions increases with time (Fig.3c). After aging for 2 s, the largest Nb difference is about 2.7%. The change rate towards the Nb-lean side is higher than that towards the Nb-rich side, due to the asymmetry of the free energy curve. For the maximum composition difference between the Nb-lean and Nb-rich regions, its change rate increases with time, because of increasing chemical driving force. After aging for 2.58 s, the maximum difference is about 10% (Fig.3d).

Then, the structural transformation from γ into α in the Nb-lean region was considered, and m_c was set as 1.32×10^{-5}. Fig.4 shows the simulated results of microstructure evolution. Two distinct evolution stages are found. The first stage presents classical morphology of spinodal decomposition (Fig. 4a). When the lowest Nb content is lower than about 0.115, the Nb-lean domains will transform into α (Fig. 4b), i.e. turning into the second stage. As the free energy derivative of α phase is

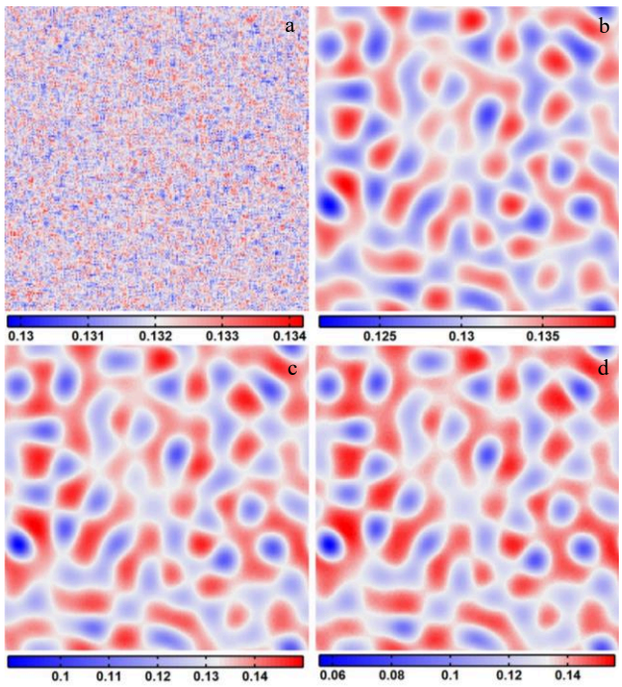

Fig.3 Simulated results of Nb content distribution for aging at the spinodal region (573 K): (a) t=0 s, (b) t=1.8 s, (c) t=2.36 s, and (d) t=2.58 s

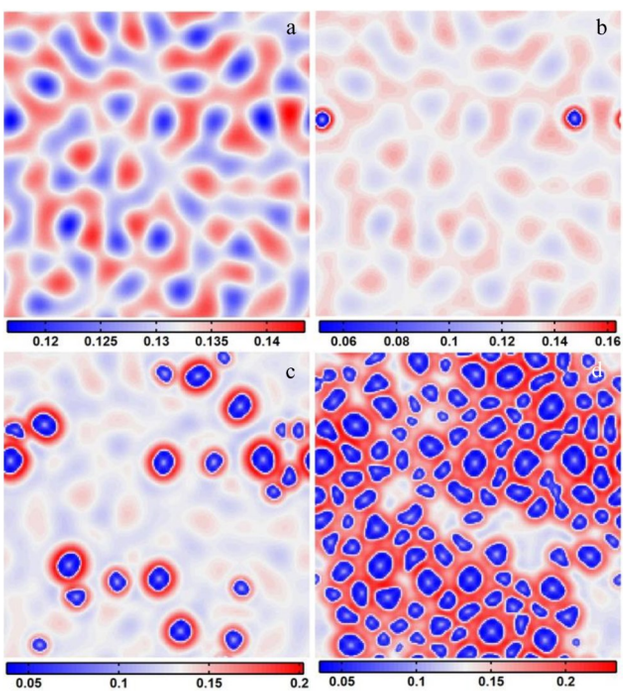

Fig.4 Simulated results of Nb content distribution at the spinodal region (573 K) when considering the precipitation of α phase: (a) t=2.13 s, (b) t=3.15 s, (c) t=2.35 s, and (d) t=2.55 s

largely higher than that of γ phase (Fig.1a), the reduction rate of Nb content in α phase is larger, and the evolution manner is similar to the nucleation-growth mode. The formed α precipitates grow with time, at the meantime, new α precipitates continuously occur (Fig. 4c). It is noted that spinodal decomposition is beneficial to the subsequent nucleation of α precipitates, and thus high nucleation rate is obtained (Fig.4d).

2.2 Aging of γ phase at the miscibility gap region

As we cannot determine which thermodynamic model is more accurate, the thermodynamic data set of Duong[8] et al is applied in this section. Based on Duong's model, U-13.2Nb alloy aged at 573 K is located in the region of coherent miscibility gap (Fig. 2b), which means that small Nb fluctuation cannot trigger Nb segregation, and the decomposition manner should belong to the classical nucleation-growth mode. Therefore, we put an embryo in the system center as the initial condition. By changing the Nb content of the embryo, it is found that the maximum Nb content for stable nucleus is about 0.119, only 0.013 lower than the matrix composition. At 573 K, the critical Nb content between α and γ phases is 0.122, which indicates that only the embryo of α phase can successfully turn into the growth stage. It is noted that this nucleation behavior is largely different from that of general precipitation. In well-known aging-hardening alloys, e. g. Al-Sc alloy[21] and Fe-Cu[22] alloy, the precipitate composition is largely different from the matrix. Obviously, small composition change is beneficial to the reduction in nucleation barrier and the increase in nucleation rate. Fig. 5 shows the simulated results of growth process. Following growth of the α precipitate, the Nb content of the adjacent matrix increases, and the precipitate composition also changes with time. At the steady growth stage, the composition change rate becomes almost constant. However,

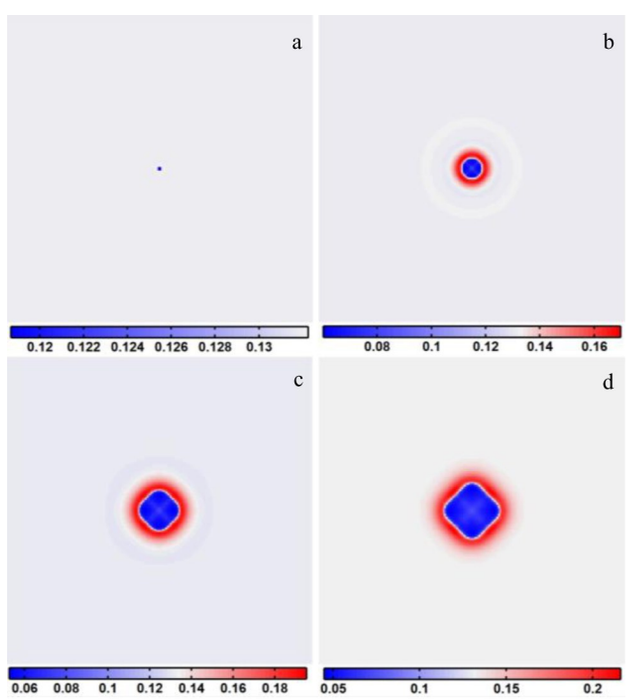

Fig.5 Simulated results of Nb content distribution during the nucleus growth process at the miscibility region (573 K): (a) t=0 s, (b) t=0.1 s, (c) t=1 s, and (d) t=3 s

the growth rate decreases with time, which may be influenced by the Nb diffusion efficiency in the precipitate and the matrix. After cooling back to room temperature, the Nb-rich domains may still maintain γ, and will not transform into α.

By introducing the seeding algorithm to the phase-field model[23], the concurrent nucleation and growth of α precipitate were simulated, and the results for different nucleation rates are shown in Fig. 6. The growth feature of individual precipitate is similar to that in Fig. 5. However, the precipitation kinetics is greatly influenced by the nucleation rate. The number of precipitates increases with nucleation rate, and the transformed fraction is also increased correspondingly. In addition, the segregation degree of Nb content is seldom influenced by the nucleation rate. The overall transformation kinetics is controlled by both the nucleation and growth rates. For the present simulations, the kinetics seems approximately linear to time.

2.3 Aging of α phase

With decrease in aging temperature, the parent phase would transform from γ to α, e. g. 423 K for U-13.2Nb alloy. According to the free energy curve (Fig. 1a), there is no doubt that α does not satisfy the condition of spinodal decomposition. For simplicity, the atomic mobility of α is set as the same as that of γ. Liu's thermodynamic model was used in this section, and the Nb content of nucleus was set as 0.17. As the matrix phase at 423 K is α phase, it can be determined from its thermodynamic curve that spinodal decomposition will definitely not occur. Therefore, the selection of thermodynamic data set will not influence the decomposition mechanism, but will influence the decomposition kinetics.

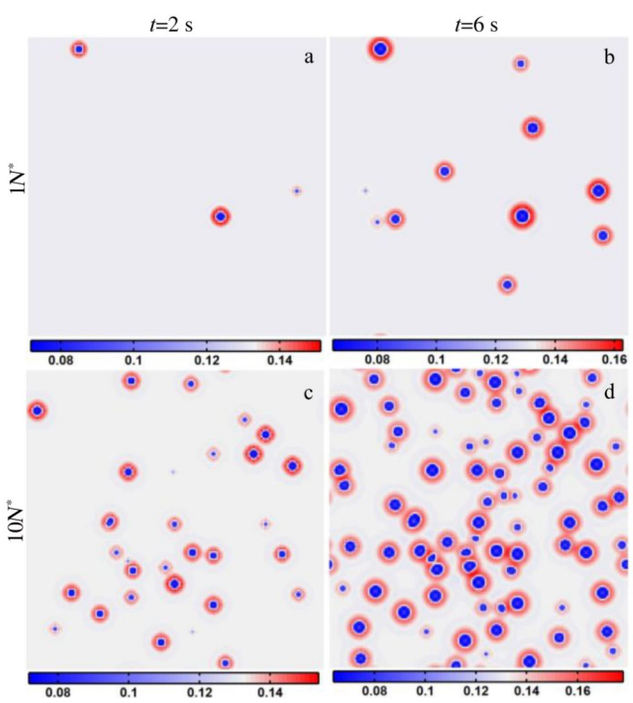

Fig.6 Simulated results of Nb content distribution for concurrent nucleation and growth at the miscibility region (573 K) (N^*= 1.25×10^{15} $m^{-2}\cdot s^{-1}$)

Three cases of different nucleation rates are simulated, and the results are shown in Fig. 7. Similar to the precipitation reaction at the γ phase (Fig. 5), the composition difference between the stable nucleus and the matrix is relatively small, smaller than 0.04 in the present case. The precipitates belong to the γ phase, their Nb content increases with time, and they are surrounded by Nb-lean domains. The transformation kinetics is greatly dependent on the nucleation rate. Besides lower decomposition kinetics influenced by temperature dependence of Nb diffusion rate, the microstructure evolution process is similar to that in Fig. 6.

3 Discussions

3.1 Nb content of precipitate

In general precipitation reactions, the composition of the precipitate is usually constant after formation of stable nucleus, and the following equilibrium condition of chemical potential is satisfied for binary system:

$$\mu_A^\alpha = \mu_A^\beta,\ \mu_B^\alpha = \mu_B^\beta \quad (9)$$

where μ is the chemical potential. Obviously, our simulated results do not satisfy this condition (Fig. 6 and Fig. 7). For the case in Fig. 6, Nb should diffuse from α to γ. Therefore, the microstructure evolution did not violate the rule that the atoms diffuse from high potential region to low potential region, but the growth of the precipitates has already occurred before the equilibrium condition is established. This phenomenon is also observed in other metallic materials, e.g. the well-known para-equilibium condition between austenite and ferrite in alloyed steels, which is resulted from the quite difference of atomic mobility between substitutional element and carbon[24–26]. One

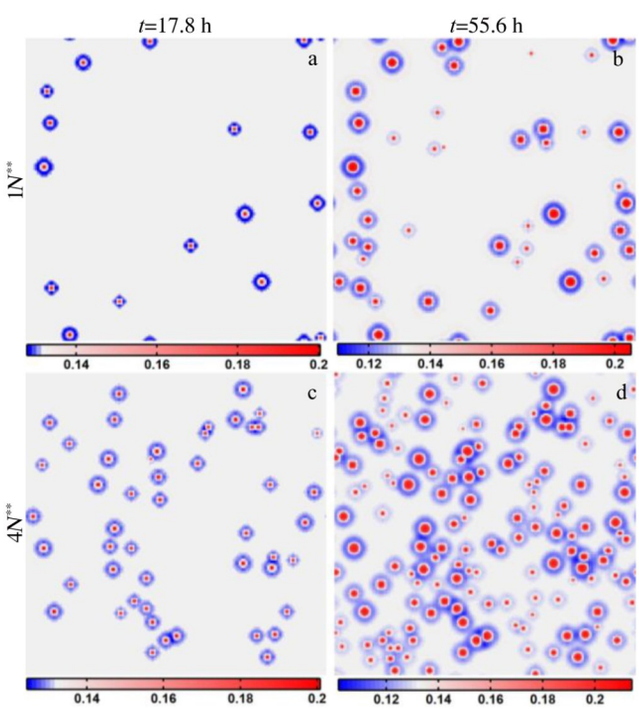

Fig.7 Simulated results of Nb content distribution for aging at the α phase region (423 K) (N^{**}=1.25×10^{12} $m^{-2}\cdot s^{-1}$)

of the reasons why the nucleus with small composition difference from matrix is stable is that there is a structural transformation ($\gamma^{\circ}\leftrightarrow\alpha''$) around the temperature range of aging, which means that a small composition change will result in the appearance of another new phase. In general precipitation reactions, this special condition does not usually exist.

In phase-field simulations, the interface migration is controlled by the term of gradient energy. The influence of gradient coefficient and the atomic mobility coefficient on the growth process was analyzed, and the results are shown in Fig.8. It can be found that with increasing gradient coefficient, the growth rate will increase, and the Nb difference is reduced. The growth rate also increases with higher coefficient of atomic mobility. However, the relationship between precipitate size and Nb difference is slightly affected by this parameter. Therefore, when the atomic diffusivity is low, e.g. at low temperatures, the Nb content of the precipitate will be largely influenced by the migration rate of the phase interface.

3.2 Influence of nucleation rate

As nucleation is the prerequisite for phase decomposition when the condition of spinodal decomposition is not satisfied, the nucleation rate plays an important role in the transformation kinetics. The case of high nucleation rate and high interface mobility was simulated, and the results are shown in Fig.9. At the early stage, the density of precipitates sharply increases, while the precipitate size is small enough. At the later stage, the nucleation rate is low because of saturation of nucleation sites, and the main change is the growth of the precipitates, following the Nb content reduction of the precipitates. After aging for 24 s, almost half regions has transformed into the α phase, but the maximum Nb difference is still low, i. e. smaller than 0.07. For the subsequent stage, the microstructure morphology changes a little, and the Nb partitioning between the Nb-lean precipitates and the Nb-rich matrix is the dominant process. This is the "uphill" diffusion between different structural phases. After cooling back to room temperature, the Nb-rich regions will not transform into the α phase. The obtained microstructure is very similar to the products of spinodal decomposition.

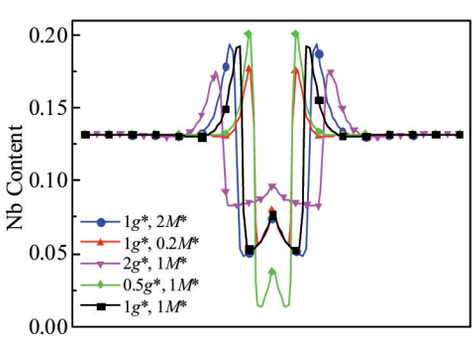

Fig.8 Distribution of Nb content after aging at 573 K for 1 s with different combinations of gradient coefficient (g*) and atomic mobility (M*) based on Duong's thermodynamic model

Therefore, sometimes it is hard to determine the detailed decomposition mechanism, i.e. spinodal or nucleation-growth.

3.3 Estimation of strengthening mechanism

One of the peculiarities of low-temperature aging effect in U-Nb alloys is that the mechanical behavior is significantly changed when no obvious microstructure change can be observed[19]. One of the possible reasons is that relatively small degree of Nb redistribution will largely raise the resistance of dislocation motion, which is responsible for plastic deformation. There are many precipitate-strengthening mechanisms, such as chemical, modulus-mismatch, coherency, stacking-fault and atomic-order strengthening. As there is no intermetallic compound for U-Nb system, the contributions of chemical, modulus-mismatch and atomic-order strengthening will be limited. In addition, it is suggested that coherency strengthening is the main strengthening mechanism. Before reaching over-aged state, the relationship between precipitate and matrix is coherent. The coherent stress, which is resulted from the dependence of lattice parameter with the solute content, is an effective obstacle to dislocation motion. The magnitude of coherent stress is approximately equal to $\eta\Delta cE'$. Based on the parameters in Table 1, the influence of Nb redistribution on the coherent stress can be obtained, i.e. σ_c=7.84Δc, which means that 1% composition difference will result in 78.4 MPa coherent stress. Compared to the critical resolved shear stress of slip and twinning modes, this level of nano-scale coherent stress will lead to obvious increase in the plastic strength without doubt.

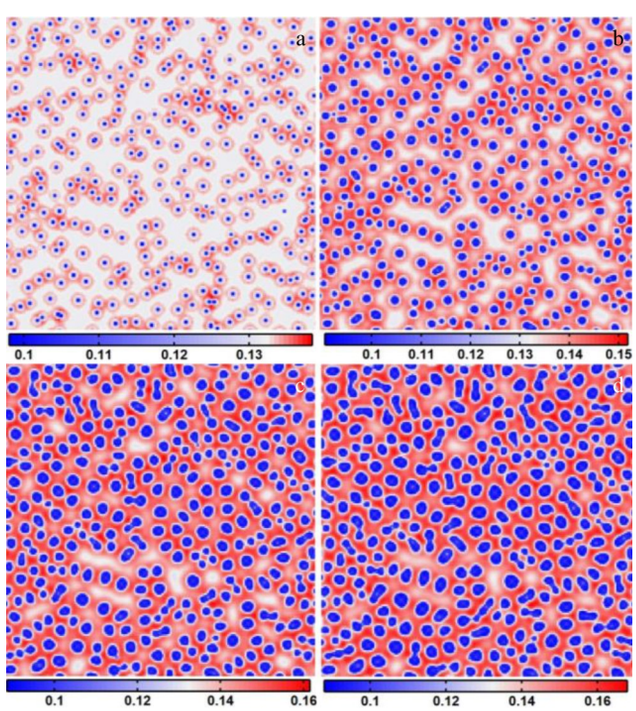

Fig.9 Simulated results of Nb content distribution (573K) for high nucleation rate and high interface mobility (N=3.3×10^{17} m^{-2}·s^{-1}, β=2×10^{-9} J/m^2): (a) t=2.4 s, (b) t=12 s, (c) t=24 s, and (d) t=36 s

For classic precipitation transition, the composition of precipitate is constant, thus the strengthening magnitude is mainly dependent on the size and amount of precipitates. However, for the non-classic precipitation transition in U-Nb alloys, the composition of precipitate will change with aging time. Taking high nucleation rate in the low temperature aging range, the strengthening magnitude will be mainly dependent on the composition difference between precipitate and matrix. The above analysis indicates that the plastic strength may be very sensitive to the Nb redistribution in U-Nb alloys.

3.4 Limitations of the present simulation

The present simulations mainly focus on the decomposition mechanism of low-temperature aging in U-Nb alloys, and the decomposition kinetics cannot be accurately described. Firstly, the thermodynamic curves of γ° and α'' phases cannot be obtained, and they are approximately treated as γ and α phases, respectively. The thermodynamic data will influence the decomposition mechanism, driving force, nucleation barrier and elastic strain energy. For example, the spinodal decomposition mechanism highly relies on the thermodynamic curve, Liu's thermodynamic data support spinodal decomposition, but Duong's thermodynamic data does not support it. It is noted that despite spinodal, non-classic nucleation-growth is the alternative mechanism, especially when aging at the α'' phase. Because the aging temperature is close to the structural transformation temperature, the composition difference between precipitate and matrix can be relatively small, which is the main reason why non-classic precipitation transition can occur in U-Nb alloys. In addition, some kinetics related parameters cannot be accurately determined, such as atomic diffusion rate, intrinsic interface migration rate and nucleation rate. Therefore, the present simulation is relatively limited on the decomposition mechanism, and the actual decomposition kinetics cannot be accurately established.

4 Conclusions

1) Compared with general precipitation, the Nb difference between stable nuclei and matrix can be relatively small in the U-13.2Nb alloy, no matter aging at the γ or α phases.

2) Competition between the intrinsic interface mobility and Nb diffusion can result in local non-equilibrium condition, and the precipitate will start to grow when its Nb content is far away from the equilibrium composition.

3) With relatively high nucleation rate and interface mobility, the decomposed microstructure is mainly nano-scale precipitates with small Nb difference from matrix, and the aging strengthening effect will be significant, even though the composition difference between Nb-lean and Nb-rich regions is relatively small.

References

1 Eckelmeyer K H, Romig A D, Weirick L J. *Metallurgical Transactions A*[J], 1984, 15: 1319

2 Xiao D, He L, Qiu Z *et al*. *Rare Metal Materials and Engineering*[J], 2018, 47(1): 363 (in Chinese)

3 Guo Y, Shuai M, Zou D *et al*. *Rare Metal Materials and Engineering*[J], 2018, 47(5): 1459 (in Chinese)

4 Sunwoo A J, Hiromoto D S. *Journal of Nuclear Materials*[J], 2004, 327(1): 37

5 Hackenberg R E, Aikin Jr R M, Kelly A M *et al*. *Microstructure and Mechanical of U-6Nb and U-8Nb in Gamma Quenched and Long-Term Aged Conditions*[R]. US: Los Alamos National Laboratory, 2016

6 Clarke A J, Field R D, Hackenberg R E *et al*. *Journal of Nuclear Materials*[J], 2009, 393(2): 282

7 Liu X J, Li Z S, Wang J *et al*. *Journal of Nuclear Materials*[J], 2008, 380(1–3): 99

8 Duong T C, Hackenberg R E, Landa A *et al*. *Calphad*[J], 2016, 55: 219

9 Mo C, Mo W, Zhou P *et al*. *Journal of Materials Science & Technology*[J], 2021, 81: 229

10 Liu Y, Yu D, Du Y *et al*. *Calphad*[J], 2012, 37: 49

11 Bian B, Zhou P, Wen S *et al*. *Calphad*[J], 2018, 61: 85

12 Chen L Q. *Annual Review of Materials Research*[J], 2002, 32: 113

13 Steinbach I. *Annual Review of Materials Research*[J], 2013, 43(1): 89

14 Wang C, Huang J, Lu Y *et al*. *Rare Metal Materials and Engineering*[J], 2019, 48(9): 2799

15 Sun Y, Zhao Y, Hou H *et al*. *Rare Metal Materials and Engineering*[J], 2018, 47(10): 3000

16 Duong T C, Hackenberg R E, Attari V *et al*. *Computational Materials Science*[J], 2020, 175: 109 573

17 Wang Y H, Zhang D C, Pi Z P *et al*. *Journal of Applied Physics*[J], 2019, 126(8): 85 102

18 Liu H, Bellón B, Llorca J. *Acta Materialia*[J], 2017, 132: 611

19 Hackenberg R E, Brown D W, Clarke A J *et al*. *U-Nb Aging Final Report*[R]. US: Los Alamos National Laboratory, 2007

20 Neumann G, Tuijin C. *Pergamon Materials Series*[J], 2008, 14: 333

21 Novotny G M, Ardell A J. *Materials Science & Engineering A*[J], 2001, 318: 144

22 Deschamps A, Militzer M, Poole W J. *ISIJ International*[J], 2001, 41(2): 196

23 Simmons J P, Wen Y, Shen C *et al*. *Materials Science and Engineering A*[J], 2004, 365: 136

24 Sietsma J, Zwaag S. *Acta Materialia*[J], 2004, 52: 4143

25 Militzer M, Mecozzi M, Sietsma J *et al*. *Acta Materialia*[J], 2006, 54(15): 3961

26 Wu H D, Miyamoto G, Yang Z G *et al*. *Acta Materialia*[J], 2018, 149: 68

U-Nb合金低温分解机制的相场法研究

崔书山，施　韬，路　超，尹嘉清，苏　斌
(中国工程物理研究院 材料研究所，四川 江油 621907)

摘　要：低温时效处理导致U-Nb合金的力学性能发生显著改变，利用相场法研究了性能变化对应的微观组织演化。结果表明，在较高温度可能发生调幅分解，但必须满足其热力学条件，而且也仅出现在初期。发生普通型析出的范围可能更广，因为合金成分接近于发生结构转变的临界成分，时效对应的母相无论是类高温立方相还是类低温正交相，稳定核胚和母相之间的Nb含量差异都可以相当小。当相界面的迁移率较大而扩散率较低时，处于长大阶段的析出物的Nb含量明显不同于平衡态成分。因此，U-Nb合金的低温时效硬化效应可能是由相分解引起的Nb再分配所导致。

关键词：U-Nb合金；低温时效；相场模拟

作者简介：崔书山，男，1992年生，博士，中国工程物理研究院材料研究所，四川 江油 621907，电话：0816-3626748，E-mail：cuishushan@caep.cn